

# Contaminant Transport in Fractured Chalk: Laboratory and Field Experiments

by K. Witthüser<sup>1</sup>, B. Reichert<sup>1</sup>, and H. Hötzel<sup>2</sup>

---

## Abstract

Laboratory experiments were performed on chalk samples from Denmark and Israel to determine diffusion and distribution coefficients. Batch tests were used to define sorption isotherms for naphthalene and *o*-xylene. Linear sorption isotherms were observed and described with Henry-isotherms. Because of the high purity and low contents of clay minerals and organic carbon, Danish and white Israeli chalk generally have low retardation capacities. Contrarily, gray Israeli chalk, with organic carbon fractions as high as 1.092%, remarkably retards organic contaminants. The  $K_{OC}$  concept is not applicable to predicting distribution coefficients based on the organic carbon content in the chalk samples. Effective diffusivities of *o*-xylene, naphthalene, and several artificial tracers were determined using through-diffusion experiments. Based on measured diffusion coefficients and available literature values, a chalk specific exponent of 2.36 for Archie's law was derived, allowing a satisfactory estimate of relative diffusivities in chalk. A field-scale tracer test with uranine and lithium was performed in the Negev desert (Israel) to examine the transferability of diffusivities determined on small rock samples in the laboratory. Due to low recovery rates of the tracer, a modified single fissure dispersion model was used for inverse modeling of the breakthrough curves. Resulting diffusivities deviate insignificantly from the laboratory values, which are considered to be representative for the investigated part of the aquifer and applicable in transport models.

---

## Introduction

Contaminant transport in chalk, as a fractured porous aquifer, occurs in both the fracture network and the porous matrix blocks. The advective-dispersive transport of contaminants through a fracture network is subject to more or less continuous interactions with the bounding matrix blocks. Matrix diffusion provides accessibility to a large volume of voids and sorption places, resulting in a large storage of solutes within the rock matrix. Even nonsorbing tracers exhibit an apparent retardation of solute transport. Both processes should be treated separately, especially because the delayed, diffusion limited sorption and desorption of solutes behave like a kinetic sorption process (Car-

ra et al. 1998). In addition to diffusion and sorption, degradation processes such as microbiological-mediated transformation can lead to significant reduction of the contaminant load. Nevertheless, degradation processes were beyond the scope of the investigations presented hereafter.

For a feasible description and prognosis of contaminant transport in fractured chalk, knowledge of the fracture network geometry, transport parameters along fractures, diffusive mass transfer between mobile and immobile water, sorption parameters related to fracture surfaces and rock matrix, as well as degradation rates are essential. Once the geological and hydrogeological settings are known, a combination of laboratory and field experiments are necessary to determine the contaminant behavior within the aquifer. Taking into account the expense of data acquisition, simple and reliable estimation procedures for the definition of transport parameters should be applied whenever possible.

Within the framework of an international joint project, an interdisciplinary research group investigated contaminant transport, monitoring techniques, and remediation strategies in European and Israeli fractured chalk.

---

<sup>1</sup>Geological Institute, University of Bonn, Nussallee 8 53115, Bonn, Germany; ++49 228 734723; fax ++49 228 734723; witthueser@uni-bonn.de

<sup>2</sup>Applied Geology, University of Karlsruhe, Germany

Received January 2002, accepted February 2003.

Copyright © 2003 by the National Ground Water Association.

This paper presents the results of laboratory experiments investigating sorption and diffusion processes in Danish and Israeli chalk and results from a field-scale tracer test. Diffusion and batch experiments were performed with selected organic contaminants and various substances, frequently used as artificial tracers in field investigations. The experimental data are used to investigate estimation procedures for sorption parameters in chalk. Diffusivities determined in the laboratory experiments are compared to values resulting from field-scale tracer experiments. Furthermore, a simple estimation procedure of diffusivities in chalk is presented. The impact of matrix diffusion on contaminant transport in chalk is interpreted with regard to monitoring strategies.

## Experiments

### Samples

Chalk samples were collected from boreholes in Sigerslev (Denmark; Maastrichtian chalk) and in the Negev desert (Israel, Eocene chalk). The Sigerslev chalk quarry (operated by Faxø Kridt A/S) is located on the Stevns peninsula on the Danish island of Zealand. The Stevns peninsula is on a local fault-bounded basement high between the eastern end of the Ringkøbing-Fyn high and the Fennoscandian Border Zone (Frykman 1994). Gently north-westward dipping Danian Bryozooan Limestone, deposited partly as mounds, crops out. The Bryozooan Limestone overlies Upper Cretaceous Chalk. On the Stevns peninsula strata of the Cretaceous-Tertiary boundary are gently folded along a northwest-southeast-trending axis resulting from a late Alpine component of compression (Nygaard 2000). Due to an axial culmination of the folds, the chalk in the Sigerslev quarry directly underlies a thin cover of Quaternary drift. A general overview of the mineralogy and facies relationships of the Chalk of northwest Europe is given in Hancock (1993).

The Israeli test site is located in the Beer Sheva syncline in the northern Negev desert (Figure 1). The axis of the syncline plunges gently toward the northeast. The test site exposes chalk formations of the lower Eocene Avdat Group. It is partly overlain by a thin Neogene and Pleistocene loess and unconsolidated sand (Nativ et al. 1995). A detailed description of the facies relationships of the Israeli chalk can be found in Benjamini (1979). The northern Negev desert has become a prime target for the siting of a variety of chemical industries. Due to the aridity of the area and the low permeability of the underlying Eocene chalk, these formations were considered to be a natural barrier to contaminant migration. The ineffectiveness of the barrier was determined in 1985, when monitoring wells were drilled (Nativ and Nissim 1992).

In order to account for their varying mineralogy and color, Israeli chalk samples were subdivided into white and gray chalk. As depicted in Table 1, significant differences in the mineralogical composition of chalk samples from Europe and Israel exist. The Israeli chalks exhibit a greater variability in terms of insoluble residue (7% to 20%) and organic carbon contents ( $f_{OC}$ ). The insoluble residue contains quartz (up to 2%), opal CT (up to 6%), the zeolite

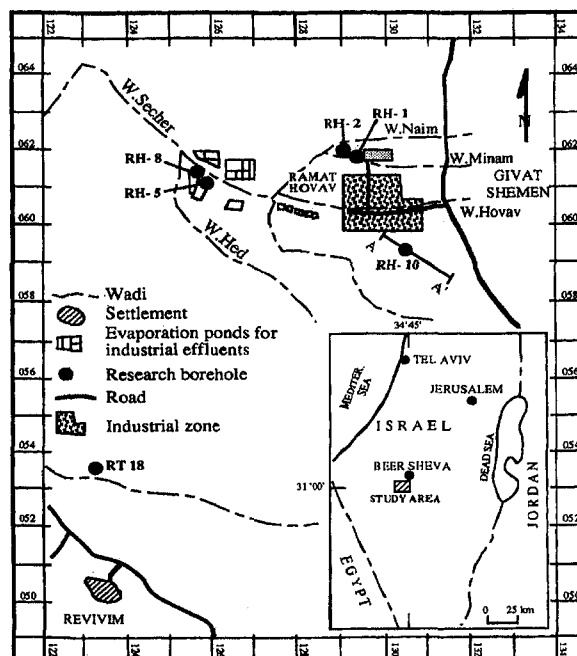


Figure 1. Location map of the Israeli study area (Nativ et al. 1995).

clinoptilolite (up to 10%), and clay minerals such as palygorskite and smectite (up to 2%). Clinoptilolite, known as an excellent ion exchanger for some inorganic contaminants, and the clay minerals present the high sorption capacities of the Israeli chalk. While the European chalk and the white Israeli chalk are characterized by low fractions of organic carbon contents, with a mean  $f_{OC}$  of 0.033% and 0.042%, respectively (Table 1), the high mean  $f_{OC}$  value of 1.092% of the gray Israeli chalk samples (Table 1) suggests a significant sorption capacity for organic contaminants. In general, the mineralogical variations reflect differences in the depositional facies.

**Table 1**  
Mineralogical Composition (Weight %) of Chalk Samples from Sigerslev (DK) and the Negev Desert (IL) (Geological Survey of the State of Israel)

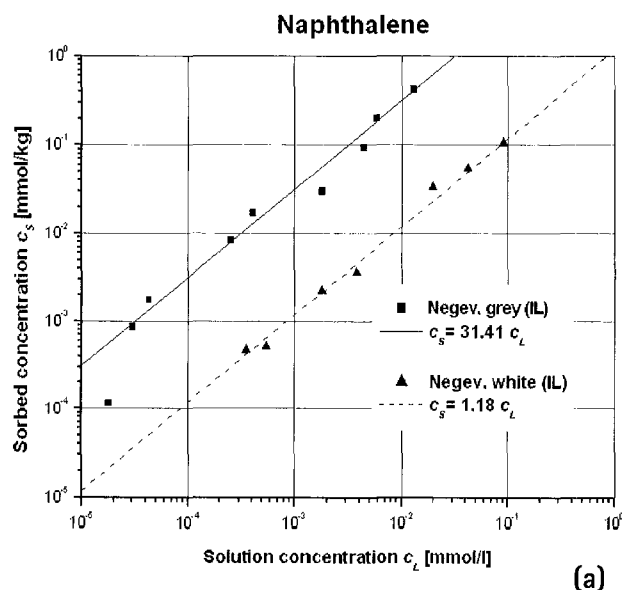
	Sigerslev (DK)	Negev, White (IL)	Negev, Gray (IL)
Calcite	98.13	80	93
Clinoptilolite	—	10	2
Quartz	0.82	2	1.6
Opal CT	—	6	1.3
Illite	0.47	—	—
Smectite and palygorskite	—	2	2
Apatite	0.59	—	—
Hematite	0.06	—	—
Rutile	0.01	—	—
$f_{OC}$	0.033	0.042	1.092

## Batch Experiments

### Experimental Method

Sorption isotherms for naphthalene and *o*-xylene in chalk were determined with batch experiments (OECD 1981). The two hydrocarbons were chosen as representatives for nonaqueous phase liquids with different transport properties. *O*-xylene is lighter than water and therefore migrates primarily to the ground water surface (LNAPL), in contrast to naphthalene which migrates predominantly to the bottom of the aquifer (DNAPL).

Batch experiments are performed to obtain distribution coefficients ( $K_d$  values) for equilibrium sorption. For equilibrium in the sorption process, all chalk samples were pulverized ( $\phi < 0.2$  mm) and batch intervals extended to 72 hours in order to exclude diffusion-limited sorption. In view of decreasing distribution coefficients with increasing solute concentrations in the batch suspension (O'Connor and Conolly 1980), a solid:solution ratio of 1:4 (2.5 g sorbent:10 mL sorbate) was chosen. This ratio yielded reproducible distribution coefficients. Furthermore, the  $K_d$  values are comparable to the rock capacity factors  $a$  (Equation 4) determined in the diffusion experiments (discussed later). Each isotherm involved at least seven interim points. Initial solution concentrations vary between 0.12 and 106 ppm for *o*-xylene and between 0.006 and 15 ppm for naphthalene. The maximum concentrations of *o*-xylene and naphthalene correspond to approximately half of their water solubility, 185 and 30 ppm, respectively. Suspensions were filled in vials and shaken in darkness at constant temperature (22°C) for 72 hours. Following shaking, phases were separated by centrifuging the vials for 45 minutes. Naphthalene was directly extracted from the solution by solid-phase microextraction (Zhang and Pawliszyn 1993; Potter and Pawliszyn 1994) and analyzed with gas chromatography-mass spectrometry. *O*-xylene was analyzed using a gas chromatograph equipped with a flame ionization detector connected to a head-space sampler. Because of technical problems, the batch experiments with naphthalene were performed only on Israeli chalk samples.



	<i>o</i> -Xylene			Naphthalene		
	$K_d$ [L/kg]	$f_{OC}$ [%]	$K_{OC}$ [L/kg]	$K_d$ [L/kg]	$f_{OC}$ [%]	$K_{OC}$ [L/kg]
Sigerslev (DK)	0.34	0.033	1030.3	—	—	—
Negev, white (IL)	0.24	0.042	571.4	1.18	0.047	2510.6
Negev, gray (IL)	22.47	1.092	2057.7	31.41	0.642	4892.5

### Sorption Parameters

The results of the batch experiments (Table 2, Figure 2) can be summarized in two general statements: (1) At low pollutant concentration (i.e., aqueous-phase concentration less than half of the solubility), sorption isotherms of hydrophobic pollutants are reported to be linear (Karickhoff 1981). In the experiments, linear-sorption isotherms were observed and therefore described with Henry-isotherms (Figure 2). (2) Because of the high purity and low contents of clay minerals and organic carbon, Danish and white Israeli chalk samples generally show low sorption capacities. In contrast, the gray Israeli chalk, with an organic carbon fraction as high as 1.092%, remarkably sorbs the organic contaminants (Table 2).

### Applicability of the $K_{OC}$ Concept in Chalk

Nonpolar hydrophobic organic compounds such as *o*-xylene and naphthalene sorb primarily on the organic carbon surfaces in the aquifer or soil material (Lambert et al. 1965; Karickhoff et al. 1979; Grathwohl 1998). This is true as long as the organic carbon content ( $f_{OC}$ ) in the aquifer medium is sufficient to neglect sorption on mineral surfaces ( $f_{OC} > 0.1\%$ ; Curtis et al. 1986; Karickhoff et al. 1979). In this case, it is possible to estimate distribution coefficients

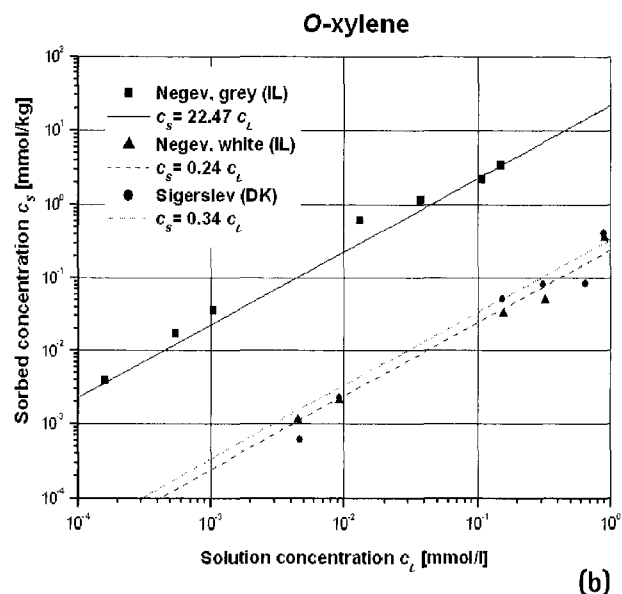


**Figure 2.** Sorption isotherms for (a) naphthalene on Israeli chalk and (b) *o*-xylene on Israeli and Danish chalk. Henry model fittings are represented by a solid (gray chalk, Israel), dashed (white chalk, Israel), and dotted (Danish chalk) line.

$K_d$  of hydrophobic organic compounds based on the organic carbon fraction  $f_{OC}$  of the aquifer and the organic carbon partition coefficients,  $K_{OC}$ , of the compound:

$$K_{OC} = \frac{K_d}{f_{OC}} \quad (1)$$

Organic carbon partition coefficients can be estimated from well-known octanol-water partition coefficients  $K_{OW}$  (Karickhoff et al. 1979; Karickhoff 1981; Means et al. 1980; Lyman et al. 1990; Schwarzenbach and Westall 1981) or water solubilities  $S_w$  (Kenega 1980; Means et al. 1980; Hassett et al. 1983). Both of these relationships are developed for soils and sediments. If they are also applicable to chalk, then time-consuming batch experiments using hydrophobic organic compounds could be avoided.

Organic carbon contents of both white Israeli chalk (0.042% and 0.047%, Table 2) and Danish chalk (0.033%, Table 2) are below the critical value ( $f_{OC} < 0.1\%$ ) for the application of the  $K_{OC}$  concept. So, for these samples, the effects of inorganic sorption/surface sorption cannot be neglected. For the two gray Israeli chalk samples, the high organic carbon content (0.642% and 1.092%, Table 2) should allow the application of a  $K_{OC}$  concept. However, experimentally derived organic carbon partition coefficients ( $K_{OC}$ ) for *o*-xylene and naphthalene (2057.7 and 4892.5 L/kg, Table 2) exceed estimations based on the octanol-water partition coefficients  $K_{OW}$  (max. 844.93 and 1380.56 L/kg, Table 3) or water solubilities  $S_w$  (max. 542.35 and 1781.92 L/kg, Table 3) by far.

Based on our results of batch experiments, the  $K_{OC}$  concept is not applicable for the prediction of distribution coefficients of organic contaminants in the investigated chalk samples. The  $K_{OC}$  concept assumes that the structure and composition of organic matter does not have any impact on the  $K_{OC}$  values. As Grathwohl (1990) and Wefer-Roehl et al. (2001) have already shown, oxidation of organic matter may result in a significant decrease of  $K_{OC}$  values. Hence, structure and composition of organic matter cannot be neglected in the prediction of geologic organic carbon partition coefficients.

**Table 3**  
Estimations of  $K_{OC}$  Values Based  
on the Octanol-Water Partition Coefficient  
 $K_{OW}$  and Water Solubility  $S_w$

Reference	<i>o</i> -Xylene	Naphtalene
	$K_{OC}$ Values [L/kg] Estimated from	$K_{OC}$ Values [L/kg] Estimated from
	$K_{OW}$ (1349)	$K_{OW}$ (2238)
Karickhoff et al. 1979	831.79	1380.56
Karickhoff 1981	561.80	927.26
Means et al. 1980	650.15	1079.08
Lyman et al. 1990	844.93	1358.32
Schwarzenbach and Westall 1981	554.13	798.07
	$S_w$ (175 mg/L)	$S_w$ (30.9 mg/L)
Kenega 1980	254.88	661.49
Means et al. 1980	542.35	1781.92
Hassett et al. 1983	362.51	1062.25

## Through-Diffusion Experiments

### Experimental Setup

Effective diffusion coefficients of naphthalene, *o*-xylene, and various tracers (Table 4) in the chalk were determined by through-diffusion experiments (Feenstra et al. 1984). The diffusive flux is observed between a reservoir cell with high concentration across a porous rock sample and a receiving cell (Figure 3) with an initial concentration of zero ( $c(t=0) = 0$ ).

Complete saturation of the 1 cm thick chalk sample slices was ensured by evacuating the samples in a desiccator before leaving them for at least two weeks in degassed water. To avoid osmotically driven fluxes, the experiments with ionic tracer were performed with rock slices saturated in an isotonic solution (Bradbury and Green 1985). These isotonic solutions were also used for the receiving cells. The diffusion cells consist of stainless steel parts, Teflon sealings, and gastight sampling systems (Teflon-lined septa, Figure 3). Each time a sample was taken from the receiving cell, the volume (4 mL) was replaced by an isotonic solution. To avoid aerobic or anaerobic degradation of the organic contaminants, the complete system (except the rock sample) was sterilized. Both reservoir and receiv-

**Table 4**  
Effective Diffusivities  $D_e$ , Rock Capacity Factors  $\alpha$ ,  
Porosities  $\epsilon$ , and Relative Diffusivities  $D'$   
in European and Israeli Chalk

	$D_e$ [m <sup>2</sup> /s]	$\alpha$ [-]	$\epsilon$ [-]	$D'$ [-]
<b>Sigerslev (DK)</b>				
Naphthalene	4.71 E-11	0.55	0.35	0.0675
<i>o</i> -Xylene	1.55 E-10	0.75	0.46	0.2158
<i>o</i> -Xylene	1.52 E-10	1.13	0.46	0.2114
Amidorhodamine G	7.57 E-11	2.90	0.51	0.2335
Deuterium	4.20 E-10	1.20	0.51	0.1972
Lithium	5.90 E-11	1.07	0.51	0.0573
Uranine	1.79 E-10	2.63	0.51	0.3971
Deuterium	3.87 E-10	1.11	0.50	0.1817
Eosine	9.39 E-11	1.20	0.50	0.2427
Sulforhodamine B	8.45 E-11	1.41	0.50	0.2724
Lithium	1.02 E-10	1.26	0.44	0.0993
Sodium naphthionate	1.31 E-10	1.59	0.44	0.2513
Pyranine	6.79 E-11	2.57	0.44	0.1651
Amidorhodamine G	6.68 E-11	1.83	0.44	0.2932
Uranine	1.32 E-10	1.50	0.44	0.2062
<b>Negev, white (IL)</b>				
Lithium	6.22 E-11	0.43	0.39	0.0604
Naphthalene	2.49 E-11	0.66	0.21	0.0357
Naphthalene	8.72 E-11	2.04	0.33	0.1249
<i>o</i> -Xylene	4.85 E-11	0.53	0.34	0.0675
<i>o</i> -Xylene	2.31 E-11	0.63	0.26	0.0322
Pyranine	1.07 E-11	1.65	0.31	0.0260
Pyranine	7.14 E-12	1.05	0.34	0.0173
Uranine	9.19 E-12	0.39	0.35	0.0204
Uranine	7.61 E-12	0.37	0.33	0.0169
Lithium	2.84 E-11	2.07	0.36	0.0275
Uranine	4.41 E-11	1.70	0.36	0.0977
<b>Negev, gray (IL)</b>				
Uranine	3.46 E-11	0.97	0.45	0.0767
Pyranine	2.78 E-11	2.40	0.44	0.0677

Italic values indicate results of multitracer experiments.

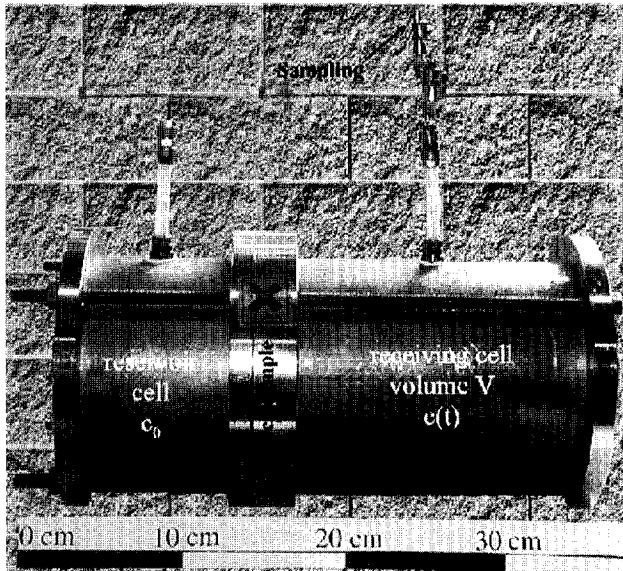


**Figure 3.** Diffusion cell used in through-diffusion experiments with organic contaminants.

ing cells were poisoned with 0.1% sodium azide and mercury chloride. At the completion of an experiment, the porosity of the chalk sample was measured by mercury injection (Table 4).

### Mathematical Description

The steady-state one-dimensional diffusive flux  $J_d$  of a solute in a porous media, due to a gradient in concentration, can be described by Fick's first law:

$$J_d = -D_e \frac{\partial c}{\partial x} = -D_p \epsilon_t \frac{\partial c}{\partial x} = -D_m \epsilon_t \frac{\delta}{\tau^2} \frac{\partial c}{\partial x} = -D_m D' \frac{\partial c}{\partial x} \quad (2)$$

where  $D_e$  is the effective diffusivity,  $D_p$  is the pore diffusion coefficient,  $\epsilon_t$  is the transport porosity,  $D_m$  is the molecular diffusivity in water,  $\delta$  is the constrictivity, and  $\tau$  is the tortuosity. The product  $\epsilon_t \delta / \tau^2$  gives the formation factor or relative diffusivity  $D'$ . It describes the diffusive properties of a rock sample independent from the molecular diffusivity of the substance under consideration. The instationary diffusive transport of a solute (assuming that sorption is reversible and linear) is described by Fick's second law:

$$(\epsilon + \rho K_d) \frac{\partial c}{\partial t} = D_e \frac{\partial^2 c}{\partial x^2} \quad (3)$$

where  $\epsilon$  is the total porosity (including dead-end pores),  $\rho$  is the bulk density of the rock sample, and  $K_d$  is the distribution coefficient. The term in parentheses on the left side is the rock capacity factor  $\alpha$ , which describes the capacity of the rock for holding a solute. For nonsorbing substances, it equals the total accessible porosity:

$$\alpha = \epsilon + \rho K_d \quad (4)$$

Breakthrough curves measured in the receiving cell were fitted with an analytical solution derived from Fick's second law for a porous slab (Carslaw and Jaeger 1959), considering the effective diffusivity  $D_e$  and the rock capacity factor  $\alpha$  as fitting parameters:

$$c(t) = \frac{A d c_0}{V} \left( \frac{D_e t}{d^2} - \frac{\alpha}{6} - \frac{2\alpha}{\pi^2} \sum_{n=1}^{\infty} \frac{(-1)^n}{n^2} \exp \left[ - \frac{D_e n^2 \pi^2 t}{\alpha d^2} \right] \right) \quad (5)$$

where  $A$  is the area and  $d$  is the thickness of the chalk disc,  $c_0$  is the concentration of the reservoir cell, and  $V$  is the volume of the receiving cell.

### Diffusion Coefficients and Rock Capacity Factors

Effective diffusivity, rock capacity factor, porosity, and relative diffusivity (Equation 2,  $D' = D_e/D_m$ ), obtained by fitting Equation 5 on experimental results, are summarized in Table 4. In general, duplication of experiments showed reproducible values. The determined effective diffusivities are generally comparable to literature values for chalk (Hill 1984; Goody et al. 1996; Grathwohl 1998). But the experimentally derived rock capacity factors show several peculiarities.

The capacity factors of pyranine clearly show a sorptive behavior ( $\alpha > \epsilon$ , Equation 4) of this tracer in the chalk. In porous and/or karstic aquifers, pyranine frequently exhibits nonsorbing transport characteristics (Käss 1998).

Almost all rock capacity factors  $\alpha$ , determined in diffusion experiments with simultaneous injection of different tracers (multitracer experiments) performed on the Danish chalk (Table 4), exceed the values of the sorptive compounds naphthalene and *o*-xylene in Danish chalk (0.55, 0.75, and 1.13, respectively). The apparently sorptive behavior of the solutes could derive from interactions of charged solutes in multitracer diffusion experiments. Those interactions might prolong the time to establish a stationary diffusive flux in the multitracer experiments. Even deuterium, which is definitely a nonreactive solute, shows a distinct retardation ( $\alpha > \epsilon$ ) in the multitracer experiments and, therefore, confirms the hypothesis. Interactions of solutes in multitracer experiments have also an impact on the observed diffusivities and will be discussed later.

Even though the diffusion experiments with *o*-xylene and naphthalene in the gray Israeli chalk were repeated twice, none was successful. No breakthrough curve of the organic contaminants in the receiving chamber could be determined. Furthermore, *o*-xylene and naphthalene concentrations in the reservoir cell were significantly decreased despite the poisoning. Such degradation of organic contaminants was not observed in the experiments with the European chalk samples and only to a minor extent in the experiments with the white Israeli chalk. Analysis of reser-

voir solution used in the naphthalene experiments with gray Israeli chalk, performed by the Institute of Biogeochemistry and Marine Chemistry (University of Hamburg), revealed naphthoquinone structures as well as salicylic acid. Naphthoquinone structures are a co-product of fungal metabolism or unspecific radical PAK-oxidation by lignin-degrading enzymes of fungi (Mahro and Kästner 1993). Salicylic acid is a central metabolite of aerobic bacterial naphthalene degradation (Grund et al. 1992). However, it was not possible to distinguish between the two possible ways of naphthalene degradation. Nevertheless, it can be concluded that the gray Israeli chalk samples contain an adopted microfauna, capable of utilizing the organic contaminants. Such microfauna are not present in the European chalk samples, but might be of interest for remediation projects if artificially introduced.

## Estimation of Diffusion Coefficients in Chalk

Effective diffusion coefficients depend on both rock and substance nature and properties. To avoid new time-consuming and expensive diffusion experiments for each substance under consideration, estimation methods for diffusivities in chalk should be applied. The relative diffusivity  $D'$  depends only on diffusion properties of the chalk sample (Equation 2). Those properties depend mainly on the total porosity and, to a negligible extent, on the mean pore-throat sizes or the pore-throat size distributions. Therefore, it is possible to estimate the relative diffusivities on the basis of the total porosities of the samples.

Several possible correlations between the relative diffusivities and porosities were tested. Among these, the frequently used Archie's law resulted in a good fit of the available data with a chalk-specific exponent of 2.36 (Figure 4). With this exponent an estimation of relative diffusivities in chalk can be easily performed:

$$D' = \epsilon^{2.36} \quad (6)$$

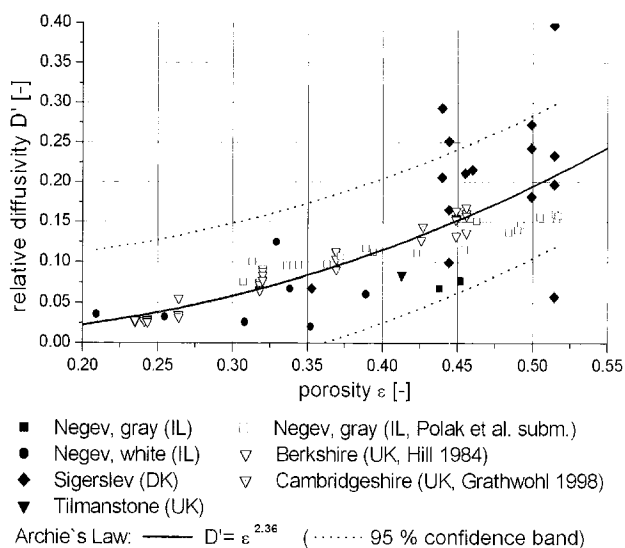


**Figure 4. Relative diffusivities versus porosities (Table 4 [solid symbols] and literature values) and fitted Archie's law with confidence bands.**

If a reduction of porosity with depth or with the distance from the fracture surface is known, this relation allows the implementation of depth-specific diffusivities.

From Figure 4, it is obvious that some of the experiments performed with Danish chalk deviate considerably, with data points outside of the 95% confidence band, from Archie's law. These points are relative to the results of multitracer diffusion experiments with Danish chalk (Table 4). While the values of the neutral deuterium in the multitracer experiments obey Archie's law, the ionic tracers show systematic deviations. The relative diffusivities of anionic tracers (uranine, pyranine, eosine, and sodium naphthionate) are generally higher; the relative diffusivities of the cation lithium are generally lower than those predicted by Archie's law. Since deuterium confirms the applicability of Archie's law, the deviations must result from the interactions between the ionic tracers. Until now, no convincing explanation has been found, but the nature of these interactions is currently under investigation.

Whether, and to what extent, diffusivities can be altered in the case of a contamination with charged contaminants is of major concern. Reduced diffusivities such as those observed for the positively charged lithium can significantly reduce the retardation capacity of the matrix and have to be taken into account for accurate transport prediction. Neglecting such enlarged diffusivities of negatively charged contaminants leads to predictions of contaminant transport that are too pessimistic and subsequent higher securities in risk analysis.

## Field Verification of Diffusion Coefficients in a Forced-Gradient Tracer Test

In general, the transferability of diffusion coefficients determined on small rock samples in the laboratory to the field scale is questionable. To check the determined diffusion coefficients in the field, a short-term forced-gradient tracer test was performed in the northern Negev desert. The experiment was conducted in white chalk with a hydraulic conductivity in the order of cm/day, a mean porosity of 35%, and a mean  $f_{OC}$  of 0.045%. A detailed description of the test site is given by Nativ et al. (1995) and Nativ et al. (1999); the latter paper also describes the drilling method of the boreholes.

The tracer test was conducted between two 3.5-inch boreholes, located at the confluence of the Wadi Naim and Wadi Hovav (Figure 1) under radial converging flow conditions. The boreholes are inclined, located 10 m apart, and were drilled normal to a northeast-southwest-striking sub-vertical major fracture system. The 24.2 m (injection borehole) and 38.8 m (extraction borehole) deep boreholes were cased only in the upper 1 to 5 m of unconsolidated sediment cover (Nativ et al. 1999). Based on information from retrieved cores, slug tests, and logs, the most permeable interval in the injection borehole (18.40 to 20.40 m below surface) was packed off prior to the tracer injection. The extraction borehole was pumped at a depth of 25 m below surface, just below the most conductive interval identified in this borehole. With this setup, the most conductive levels of the two boreholes coincide, taking the surface topography into account. A direct connection of the boreholes by

a fracture system was assumed. A preliminary pumping test confirmed the hydraulic connectivity between the boreholes.

A natural hydraulic head gradient of 0.012 was measured between the boreholes. For the experiment, the hydraulic head gradient was increased up to 0.028 by an extraction of 0.88 L/min. After establishing steady-state flow conditions, 5 g of uranine and 500 g of LiCl (equal to 81.84 g lithium) were dissolved in 2 L of water from the field site and injected into the bottom of the packer interval with a volume of ~12.5 L. To avoid an increase of the hydraulic head in the packer interval during tracer injection, 2 L of water was simultaneously pumped from its top using small 12 V pumps. Finally, 2 L of the previously withdrawn water from the packed interval were used to flush the tracer solution from the injection tube into the packer interval. During the flush, the hydraulic head gradient increased up to 0.058. Within 12 minutes, the head decreased to the previous level. Variations of hydraulic head gradients were neglected in the analysis. The injection process lasted less than 3 minutes, which can be assumed to be instantaneous with respect to the mean residence times of the tracers (~170 minutes, Table 5). Samples were analyzed for lithium using atomic adsorption (Ben-Gurion University of the Negev) and for uranine by fluorescence spectrophotometry (Hebrew University of Jerusalem).

The simultaneous injection of two tracers with different molecular diffusion coefficients, uranine (4.51 E-10 m<sup>2</sup>/sec) and lithium (1.03 E-9 m<sup>2</sup>/sec), allowed the evaluation of the diffusion properties characterizing the chalk matrix. The first arrival (~2 hours) and peak times (4 hours) of uranine and lithium are almost identical (Figure 6). Both tracers have very low recovery rates with 4.37% of uranine and 4.97% of lithium. The low recovery is a result of transversal dispersivity, wellbore storage of the tracers, tracer loss by downstream migration due to an insufficient extended capture zone of the recovery well and/or movement of tracers into stagnant volumes of water. Only the tailing part of the breakthrough curves (BTCs, Figure 6) exhibit small variations. To interpret the BTCs with respect to matrix diffusion, the tailing effects of the BTCs have to be characterized. For example, Becker and Shapiro (2000) reported extended tailing in tracer tests conducted in fracture networks in crystalline rock that were not caused by diffusion processes. They hypothesized an advection-dominated tailing caused by spatial and temporal heterogeneous transport in the fractured rock. Witthüser

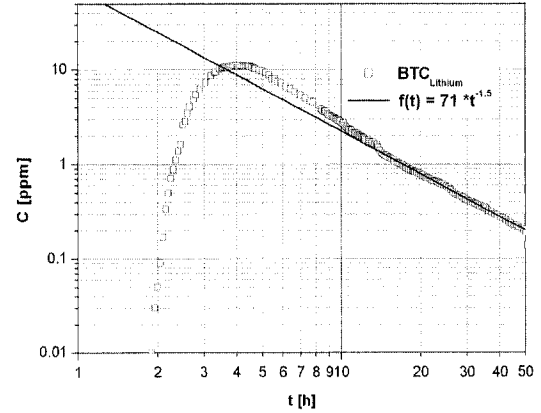


**Figure 5. Log-log plot of the observed lithium breakthrough curve (BTC<sub>Lithium</sub>).**

(2001) observed extended tailings in tracer tests conducted in an ore dyke due to wellbore storage of tracers. Nevertheless, due to the high matrix porosity of the chalk a diffusion-controlled tailing can be expected, even for short-distance tracer tests. A diffusion-determined tailing can be identified by a decrease in the concentration of the tailing according to  $t^{-1.5}$  (Tsang 1995). This criteria allows a distinction to be observed between an injection- or dispersion- and diffusion-determined tailing (Witthüser 2001).

For the Israeli test site, both BTCs (Figure 5) satisfy the criteria. Therefore, a double-porosity model with a single rate of diffusion, e.g., the single fissure dispersion model (SFDM; Maloszewski and Zuber 1985), can be applied.

However, due to the low recovery rate of the tracers, several complementary assumptions are needed to apply the SFDM model (Maloszewski 2002). Assuming that transversal dispersion cannot be neglected, a transversal dispersion term  $g(\alpha_i)$  is included in the SFDM:

$$C(t) = \frac{a M}{2\pi Q} \sqrt{Pe t_0} \int_0^t \exp \left[ -\frac{Pe(t_0 - \tau)^2}{4t_0 \tau} - \frac{(\tau a)^2}{(t - \tau)} \right] \frac{d\tau}{\sqrt{\tau(t - \tau)^3}} g(\alpha_i) \quad (7)$$

where  $a$ ,  $Pe$ , and  $t_0$  are the fitting parameters of the SFDM (Equations 10 through 12),  $M$  is the injected mass, and  $Q$  is the flow rate.

The maximal concentration  $c_{\max}$  of the breakthrough curve at the time  $t_{\max}$  is given by

$$C(t_{\max}) = \frac{a M}{2\pi Q} \sqrt{Pe t_0} \int_0^{t_{\max}} \exp \left[ -\frac{Pe(t_0 - \tau)^2}{4t_0 \tau} - \frac{(\tau a)^2}{(t - \tau)} \right] \frac{d\tau}{\sqrt{\tau(t - \tau)^3}} g(\alpha_i) \quad (8)$$

$$= C_{\max}$$

<b>Table 5</b> <b>Fitting Parameter of the SFDM</b> <b>(<math>Pe</math>, <math>t_0</math>, and <math>a</math>) and Derived Physical</b> <b>Parameters (<math>2b</math>, <math>\alpha_i</math>, and <math>D_e</math>)</b>			
		Uranine	Lithium
$Pe$	[-]	90	100
$t_0$	[s]	10400	10000
$a$	[s <sup>-0.5</sup> ]	0.0058	0.0075
$2b$	[μm]	397	405
$\alpha_i$	[m]	0.11	0.11
$D_e$	[m/s <sup>2</sup> ]	1.51 E-11	2.62 E-11

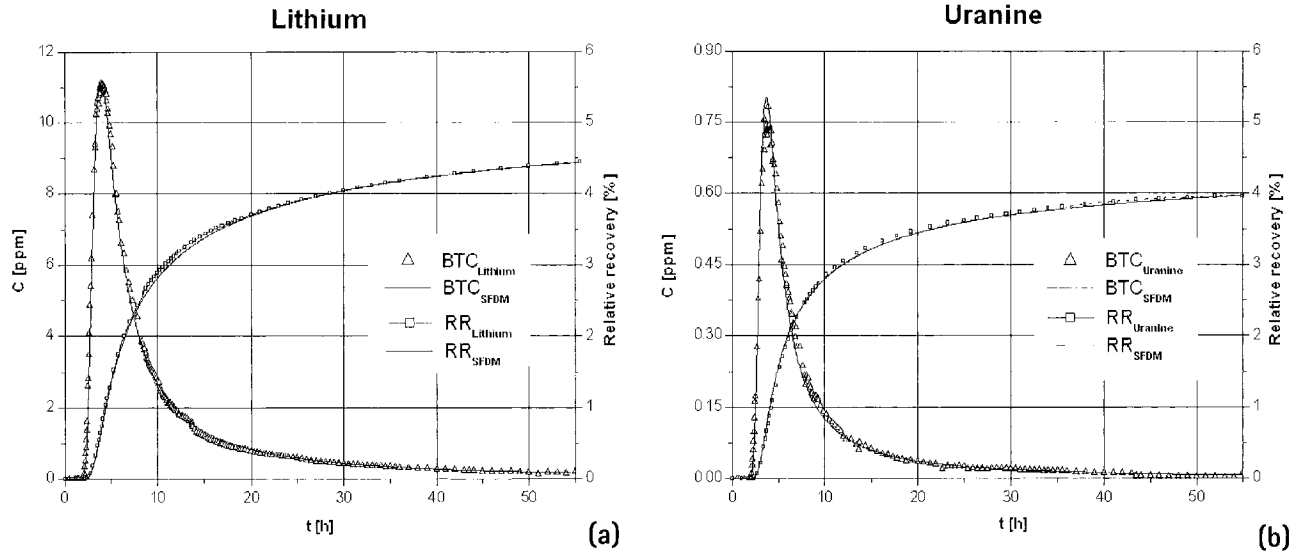


**Figure 6.** Best fit ( $BTC_{SFDM}$ ) of the observed (a) lithium and (b) uranine breakthrough curves (BTC) and corresponding relative recovery curves (RR). A constant background concentration of 170 mg/L was subtracted from the (a) lithium BTC.

Division of Equations 7 and 8 eliminates the dispersion term  $g(\alpha_i)$  as well as  $M$  and  $Q$ :

$$C(t) = c_{\max} \frac{\int_0^t \exp\left[-\frac{Pe(t_0 - \tau)^2}{4t_0\tau} - \frac{(\tau a)^2}{(t - \tau)}\right] \frac{d\tau}{\sqrt{\tau(t - \tau)^3}}}{\int_0^{t_{\max}} \exp\left[-\frac{Pe(t_0 - \tau)^2}{4t_0\tau} - \frac{(\tau a)^2}{(t - \tau)}\right] \frac{d\tau}{\sqrt{\tau(t - \tau)^3}}} \quad (9)$$

With Equation 9, a SFDM can be applied despite low recovery rates in the tracer test. Nevertheless, the assumption that the injection and extraction borehole intersect the same streamline has to be proved. In the present tracer test between two boreholes intersecting the same fracture system, this assumption seems to be quite reasonable.

The three fitting parameters of the SFDM ( $a$ ,  $Pe$ ,  $t_0$ ) combine several physical parameters. For nonreactive tracers the diffusion parameter  $a$  is given by (Maloszewski 1994):

$$a = \frac{\varepsilon \sqrt{D_p}}{2b} \quad (10)$$

where  $2b$  is the mean fracture aperture. The Peclet number  $Pe$  is a measure of the relative importance of advection to (longitudinal) hydrodynamic dispersion  $D_{hl}$  and is defined by

$$Pe = \frac{vX}{D_{hl}} = \frac{vX}{D_m + \alpha_l v} \quad (11)$$

where  $v$  is the mean flow velocity,  $X$  is the distance along the flow direction between the injection and extraction borehole, and  $\alpha_l$  is the longitudinal dispersion length.

The mean travel time  $t_0$  of mobile water or a nonsorbing tracer in the fracture is given by

$$t_0 = \frac{X}{v} \quad (12)$$

The measured tracer breakthrough curves allowed the determination of several transport parameters by inverse modeling with the SFDM (Figure 6, Table 5). This inverse modeling yielded effective diffusion coefficients of  $1.51 \text{ E-11 m}^2/\text{sec}$  (uranine) and  $2.62 \text{ E-11 m}^2/\text{sec}$  (lithium). These effective diffusivities are in good agreement with the values determined with the laboratory experiments performed on white chalk samples from the Israeli test site (compare Table 4). Provided that the modified SFDM is appropriate to model the field scale tracer test, diffusivities determined in the laboratory are representative for the investigated part of the aquifer and applicable in transport models.

## Implications for Monitoring and Remediation Strategies

Based on the results of this study, several conclusions may be drawn with regard to monitoring strategies and remediation measures in high-porosity chalk aquifers. Consider a scenario of a contaminant input of several years duration into a fractured chalk aquifer followed by removal of the source. Due to matrix diffusion it may take several decades to observe the reduced maximum concentration at a sampling point only 100 m downstream. The higher the matrix porosity, the larger the retardation and reduction in maximum concentration. An even longer delay may be caused by additional retardation due to sorption or to misplaced observation boreholes not intersecting a transmissive fracture.

To obtain contaminant input, at least one sampling point should be in the contaminant source itself or directly downstream. The assessment of contamination should include the concentrations of the mobile fracture water as well as the concentrations in the stagnant matrix water, i.e., the stored and not directly accessible mass of contaminants. This can be done in situ with suction cups or off-site with core spinning. The evaluation of mobile water concentrations have to consider the long breakthrough times, which



can easily be masked by temporal or seasonal variations. For this reason, they should be based on long-time series, which increase with distance from the source. The interpretation of mobile water concentrations and calculations of input concentrations or plume development have to take matrix diffusion into account. A concentration profile within the matrix might help to reconstruct the development of the contamination. The essential diffusion coefficients can be easily estimated according to Archie's law with a chalk specific exponent of 2.36.

The slow diffusive release of contaminants into the mobile fracture water has strong implications for remediation measures. The only feasible way to remediate a contamination in highly porous hardrock aquifers would appear to be low-energy remediation schemes such as reactive walls in porous aquifers. To make use of similar in situ techniques for diffusive plumes in fractured rocks, artificial drain elements should be used to channel the flow to special in situ treatment sections ("catch and treat"). Depending on the degree of flow channeling and the orientation of the fracture pattern, this can be done by using an artificially induced fracture network, by line cutting, or by horizontal drilling. An X- or Y-shaped configuration is recommended, using the upstream part for collecting the ground water flow and the downstream part for distributing the water. In the central part, an in situ treatment system could be installed.

A comparable concept, the so-called refractive flow and treatment (RFT) system, has already been recommended by Dick and Edwards (1997) and patented in 1998. Their modular system consists of high-permeability collection cells, in situ permeable treatment zones, and high permeable dispersal cells. The applicability of these concepts was proven by analytical and numerical modeling (Edwards et al. 2001), and field tests are planned. For the moment, catch-and-treat (especially RFT) concepts seem to be the most promising approach to remediate contamination in highly porous fractured aquifers of low to moderate permeability.

## Acknowledgments

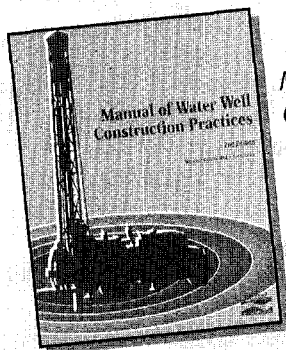
The work was supported by the EC under ENV4-CT97-0441. The assistance of Dr. R. Nativ and Dr. E. Adar, who enabled and helped us to perform the tracer test, Dr. J. Bloomfield, BGS, who performed a part of the mercury-injection porosity measurements, and W. Stichler, GSF, who performed the isotope analysis, is gratefully acknowledged. The authors wish to thank W. Kelly and S. Brouyère for their useful comments to improve the paper.

## References

- Becker, M.W., and A.M. Shapiro. 2000. Tracer transport in fractured crystalline rock: Evidence of nondiffusive breakthrough tailing. *Water Resources Research* 36, no. 7: 1677–1686.
- Benjamini, C. 1979. Facies relationships in the Avedat Group (Eocene) in the northern Negev, Israel. *Israel Journal of Earth-Sciences* 28, 47–69.
- Bradbury, M.H., and A. Green. 1985. Measurement of important parameters determining aqueous-phase diffusion rates through crystalline rock matrices. *Journal of Hydrology* 82, 39–55.
- Carrera, J., X. Sánchez-Vila, I. Benet, A. Medina, G. Galarza, and J. Guimerà. 1998. On matrix diffusion: Formulations, solution methods and qualitative effects. *Hydrogeology Journal* 6, no. 1: 178–190.
- Carslaw, H.S., and J.C. Jäger. 1959. *Conduction of Heat in Solids*. Oxford, U.K.: Clarendon Press.
- Curtis, P.G., M. Reinhard, and P.V. Roberts. 1986. Sorption of hydrophobic organic compounds by sediments. In *Geochemical Processes at Mineral Surfaces*, ed. J.A. Davis, and K.F. Hayes, 191–216. Washington, D.C.: American Chemical Society.
- Dick, V.B., and D.A. Edwards. 1997. Refractive flow and treatment for passive ground water remediation in bedrock: An analog to funnel-and-gate technology. In *Proceedings of the 1997 International Containment Technology Conference and Exhibition*, 459–466. Tallahassee, Florida: International Cooperative Environmental Research.
- Edwards, D.A., V.B. Dick, J.W. Little, and S.L. Boyle. 2001. Refractive flow and treatment systems: Conceptual, analytical, and numerical modeling. *Ground Water Monitoring & Remediation* 21, no. 3: 64–70.
- Feenstra, S., J.A. Cherry, E.A. Sudicky, and Z. Haq. 1984. Matrix diffusion effects on contaminant migration from an injection well in fractured sandstone. *Ground Water* 22, no. 3: 307–316.
- Frykman, P. 1994. Variability in petrophysical properties in U. Maastrichtian Chalk outcrops at Stevns, Denmark. DGU Service Report 38.
- Goody, D.C., D.G. Kinniburgh, and J.A. Barker. 1996. Development of a rapid method for determining apparent diffusion coefficients for chloride in chalk. British Geological Survey Technical Report WD/95/66.
- Grathwohl, P. 1990. Influence of organic matter from soils and sediments from various origins and the sorption of some chlorinated aliphatic hydrocarbons: Implications on  $K_{OC}$  correlations. *Environmental Science and Technology* 24, no. 11: 1687–1693.
- Grathwohl, P. 1998. *Diffusion in Natural Porous Media: Contaminant Transport, Sorption/Desorption and Dissolution Kinetics*. London: Kluwer Academic.
- Grund, E., B. Denecke, and R. Eichenlaub. 1992. Naphtalene degradation via salicylate and gentisate by *Rhodococcus* sp. Strain B4. *Applied Environmental Microbiology* 58, 1874–1877.
- Hancock, J.M. 1993. The formation and diagenesis of chalk. In *The Hydrogeology of the Chalk of North-West Europe*, ed. R.A. Downing, M. Price, and G.P. Jones, 14–34. Oxford, U.K.: Clarendon Press.
- Hassett, J.J., W.L. Banwart, and R.A. Griffin. 1983. Correlation of compound properties with sorption characteristics of nonpolar compounds by soil and sediments. In *Environment and Solid Waste: Characterization, Treatment and Disposal*, ed. C.W. Francis and S.I. Auerbeck, 161–172. London: Butterworth Publishers.
- Hill, D. 1984. Diffusion coefficients of nitrate, chloride, sulphate and water in cracked and uncracked chalk. *Journal of Soil Science* 35, 27–33.
- Käss, W. 1998. *Tracing Technique in Geohydrology*. Rotterdam, Netherlands: Balkema.
- Karickhoff, S.W. 1981. Semi-empirical estimation of sorption of hydrophobic pollutants on natural sediments. *Chemosphere* 10, 833–846.
- Karickhoff, S.W., D.S. Brown, and T.A. Scott. 1979. Sorption of hydrophobic pollutants in sediment suspension. *Water Research* 13, no. 3: 241–248.
- Kenaga, E.E. 1980. Predicted bioconcentration factors and soil sorption coefficients of pesticides and other chemicals. *Ecotoxicology and Environmental Safety* 4, 26–38.
- Lambert, S.M., P.E. Porter, and R.H. Schieferstein. 1965. Movement and sorption of chemicals applied to soil. *Weeds* 13, 185–190.

- Lyman, W.J., W.F. Reehl, and D.H. Rosenblatt. 1990. *Handbook of Chemical Property Estimation Methods*. Washington, D.C.: American Chemical Society.
- Mahro, B., and M. Kästner. 1993. Der mikrobielle Abbau polyzyklischer aromatischer Kohlenwasserstoffe (PAK) in Böden und Sedimenten: Mineralisierung, Metabolitenbildung und Entstehung gebundener Rückstände. *BioEngineering* 9, 50–58.
- Maloszweski, P. 2002. Institute of Hydrology, Munich-Neuherberg, Germany, personal communication.
- Maloszweski, P. 1994. Mathematical modelling of tracer experiments in fissured rocks. *Freiburger Schriften zur Hydrologie* 2. Freiburg i. Breisgau.
- Maloszewski, P., and A. Zuber. 1985. On the theory of tracer experiments in fissured rocks with a porous matrix. *Journal of Hydrology* 79, 333–358.
- Means, J.C., S.G. Wood, J.J. Hassett, and B.L. Banwart. 1980. Sorption of polynuclear hydrocarbons by sediments and soils. *Environmental Science and Technology* 21, no. 11: 1524–1528.
- Nativ, R., and I. Nissim. 1992. Characterization of desert aquitard: Hydrologic and hydrochemical considerations. *Ground Water* 30, no. 4: 598–606.
- Nativ, R., E. Adar, O. Dahan, and M. Geyh. 1995. Water recharge and solute transport through the vadose zone of fractured chalk under desert conditions. *Water Resources Research* 31, no. 2: 253–261.
- Nativ, R., E.M. Adar, and A. Becker. 1999. Designing a monitoring network for contaminated ground water in fractured chalk. *Ground Water* 37, no. 1: 38–47.
- Nygaard, E. 2002. Geological Survey of Denmark and Greenland, personal communication.
- O'Connor, D.J., and J.P. Connolly. 1980. The effect of the concentration of adsorbing solids on the partition coefficient. *Water Research* 14, 1517–1523.
- Organisation for Economic Cooperation and Development. 1981. *OECD Guideline for Testing of Chemicals, No. 106: Adsorption/Desorption*. Paris, France: OECD.
- Polak, A., R. Nativ, and R. Wallach. Diffusion coefficient of chalk and its correlation to porosity. *Ground Water*, submitted.
- Potter, D.W., and J. Pawliszyn. 1994. Rapid determination of polyaromatic hydrocarbons and polychlorinated biphenyls in water using solid-phase microextraction and GC/MS. *Environmental Science and Technology* 28, no. 2: 298–305.
- Schwarzenbach, R.P., and J. Westall. 1981. Transport of nonpolar organic compounds from surface water to ground water: Laboratory sorption studies. *Environmental Science and Technology* 15, no. 11: 1360–1367.
- Tsang, Y.W. 1995. Study of alternative tracer tests in characterizing transport in fractured rocks. *Geophysical Research Letters* 22, no. 11: 1421–1424.
- Wefer-Roehl, A., E.R. Graber, M.D. Borisover, E. Adar, R. Nativ, and Z. Ronen. 2001. Sorption of organic contaminants in a fractured chalk formation. *Chemosphere* 44, no. 5: 1121–1130.
- Witthüser, K. 2001. Untersuchungen zum Stofftransport in geklüfteten Festgesteinen unter besonderer Berücksichtigung der Matrixdiffusion. Ph.D. thesis, Department of Applied Geology, University of Karlsruhe, Karlsruhe, Germany.
- Zhang, Z., and J. Pawliszyn. 1993. Headspace solid-phase microextraction. *Analytical Chemistry* 65, no. 14: 1843–1852.

## Learn the latest in water well construction practices!



### *Manual of Water Well Construction Practices*

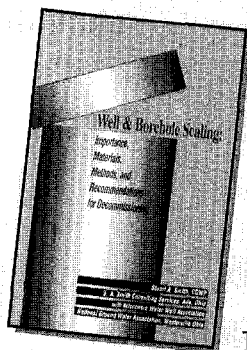
Edited by Stuart Smith  
NGWA

Four years in the making, this book is a revision of a document originally written under contract for the U.S. EPA. Comprehensive in its scope of current well construction methods, it is designed to serve not only contractors but as a guideline for state well inspectors.

Reference# T871

NGWA member price: \$25

Prospective member price: \$31.25



### *Well and Borehole Sealing: Importance, Materials, Methods, and Recommendations for Decommissioning*

by Stuart Smith  
Wisconsin Water Well Association  
NGWA

This illustrated book features discussions of the differences between well abandonment and well sealing, avoiding failures and faults in borehole grout seals, choices in sealing materials, site preparation, emplacement procedures and requirements, and more. An appendix provides excellent ready-reference tables on grouts and grout use. The 30 illustrations found throughout the book clearly explain the procedures and benefits of proper abandonment and sealing.

Reference# T345

NGWA member price: \$15

Prospective member price: \$18

For additional information on these titles, or any of the other titles offered through the NGWA Bookstore, call our Customer Service Department at 1-800-551-7379, or visit us on the web at [www.NGWA.org](http://www.NGWA.org).